buildings

MDPI

Article

Investigation of an Empirical Creep Constitutive Model of Changsha Red Loam

Lin Long [1], Zhida Li [1] and Yunyu Li [2,*]

[1] School of Naval Architecture, Ocean and Energy Power Engineering, Wuhan University of Technology, Peace Avenue 1178, Wuhan 430063, China; l_lin152@163.com (L.L.); zhidali@163.com (Z.L.)
[2] School of Transportation and Logistics Engineering, Wuhan University of Technology, Peace Avenue 1178, Wuhan 430063, China
* Correspondence: liyunyu@whut.edu.cn

Abstract: To describe and predict the creep deformation of Changsha red loam (including sandy soil and silty clay) in China, an empirical creep model was proposed based on a laboratory consolidation compression test. Two classical soil layers were sampled from the deep foundation pit site and fourteen samples were designed for tests under different loading conditions. Results show that the deformation process illustrates deceleration and stabilization creep with its vertical load lower than 500 kPa, while it may illustrate acceleration with its vertical load higher than 500 kPa. By analyzing the experimental results, the empirical creep model of the red loam was established. Adopting the model to predict the deformation of red loam shows the prediction curves match the actual situation, proving that the model plays a significant role in predicting the creep deformation of Changsha red loam.

Keywords: consolidation test; creep model; constitutive relation; nonlinearity; deformation prediction

check for updates

Citation: Long, L.; Li, Z.; Li, Y. Investigation of an Empirical Creep Constitutive Model of Changsha Red Loam. *Buildings* **2023**, *13*, 1064. https://doi.org/10.3390/buildings13041064

Academic Editor: Suraparb Keawsawasvong

Received: 8 March 2023
Revised: 13 April 2023
Accepted: 15 April 2023
Published: 18 April 2023

Copyright: © 2023 by the authors. Licensee MDPI, Basel, Switzerland. This article is an open access article distributed under the terms and conditions of the Creative Commons Attribution (CC BY) license (https://creativecommons.org/licenses/by/4.0/).

1. Introduction

The soil is a viscoelastoplastic body with certain creep characteristics, in which compression deformation arises with the condition of constant effective stress and enduring time. Meanwhile, different soil components, stress history, and temperature change show different creep states [1]. In practical engineering, creep deformation of soil will occur with long-term load, which will adversely affect the stability of the deep foundation pit and the safety of infrastructure, so it is necessary to consider the negative effects of soil creep. A number of research studies, referring to creep characteristics and models of soil, have been carried out in China and overseas. Based on the Burgers model, which can reflect the creep characteristics of soft rock in the saturation-loss cycle, Li, A.R., et al. [2] established the creep damage constitutive of silty mudstone by introducing a fractional order Abelian clay pot and aging factor. Michael, L., et al. [3] studied a soft soil creep constitutive model that can predict the settlement displacement of a Swedish peat embankment. Ofrikhter, V.G., et al. [4] looked at the soft soil creep constitutive model to describe the stress–strain relationship of municipal solid waste. Huang, W., et al. [5] analyzed the viscoelastic-plastic deformation of Marine sedimentary soft soil in Shenzhen through lateral unloading creep tests under different excess pore water pressures, proposing a lateral unloading creep model of soft soil based on the modified merchant model. Based on the Kelvin Voigt model, Zhang, Z., et al. [6] studied the viscoelastic creep model of frozen soil through the spherical indentation test, uniaxial creep test, and triaxial creep test. Wang, P., et al. [7] studied the macro and micro unified creep constitutive model of frozen soil by conducting creep tests under the conditions of constant temperature and variable temperature, taking the effects of temperature and stress levels into account. Hou, F., et al. [8] conducted triaxial creep tests on frozen silty clay with different coarseness contents, introduced hardening variables

and damage variables to improve the Nishihara Masao model, and proposed a constitutive model that can describe the whole process of artificial frozen soil creep. With the triaxial creep test, Hu, Z.Q., et al. [9] analyzed the creep characteristics of artificially prepared soil at the site and studied a semi-empirical and semi-theoretical viscoelastoplastic creep constitutive model that can describe the nonlinear characteristics of soil. Yu, H.D., et al. [10] conducted consolidation creep tests on clay rocks, analyzed the creep characteristics under the coupled seepage and stress conditions, and proposed a one-dimensional creep constitutive model that can describe the mechanical properties of clay rocks. Based on laboratory triaxial creep tests, Liu, J., et al. [11] proposed a creep constitutive model suitable for describing the creep characteristics of pebble soil.

Large numbers of engineering practices and laboratory creep tests illustrate that soil creep has nonlinear characteristics described by the empirical creep model [12]. For instance, the typical representatives of traditional empirical creep models are the Singh–Mitchell Model [13] and Mesri Model [14]. While there are many existing models describing the creep behavior of soils, they are not fully in tune with the actual monitoring results of the deep foundation pit due to the dispersion, regionalism, and variability of soils. Thus, for the purpose of studying the creep characteristics of Changsha red loam accurately, it is essential to establish a corresponding creep constitutive model based on a consolidation compression test.

In this paper, an empirical creep model is proposed based on the creep test data, which can be applied to describing and predicting nonlinear characteristics of red loam. The research provides important guidance for the construction of empirical constitutive models of soils in other regions.

2. Consolidation Creep Test of Changsha Red Loam

2.1. Test Sample

The consolidation creep test is based on the deep foundation pit project of the World Trade Group (WTG). As shown in Figure 1 [15,16], the Project is located on the west side of Yinpenling Bridge in Changsha nearby, and adjacent to Binjiang-Jinzuo in the east, Yuebei Road in the west, and Yuelu Avenue in the south. The length of the foundation pit is 162 m, the width is 67~84 m, and the maximum excavation depth is 19.90 m. The soil of the excavation site is a typical type of Changsha red loam and the specific physical and mechanical properties are listed in Table 1. Soil samples used in the test were taken from No. III and No. IV soil layers with a depth of 6–14 m. Windproof and dry measures should be taken in the process of preparing and transporting soil samples to ensure the original state of soil to the greatest extent.

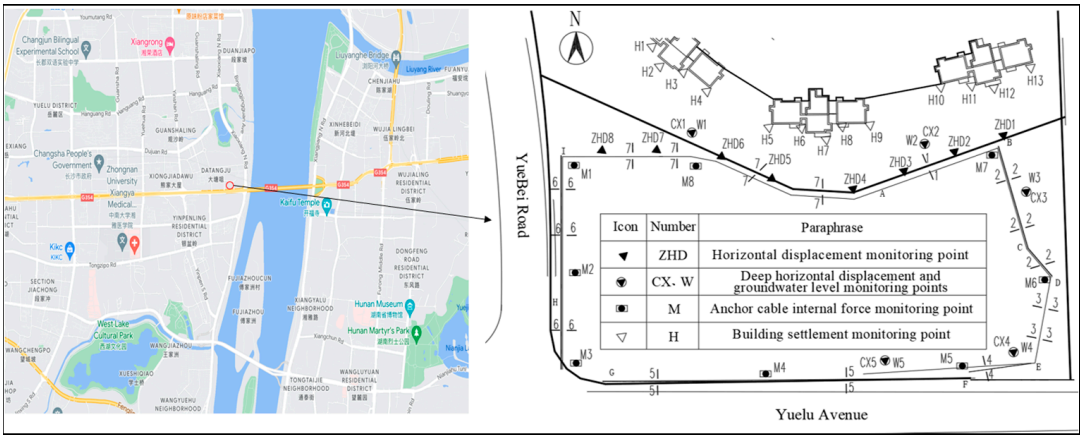


Figure 1. Location of foundation pit.

Table 1. Physical and mechanical characteristics of soil samples.

Soil Layer	Modulus of Compression E_s/MPa	Natural Gravity γ/(kN/m^3)	Soil Thickness /m	Internal Friction Angle φ/°	Cohesion c/kPa	Poisson's Ratio
No. III Sandy soil	10.93	21.1	5.90–11.20	35	30	0.32
No. IV Silty clay	8.60	20.3	10.70–14.78	20	30	0.30

2.2. Test Instrument

According to the Standard for Geotechnical Test Methods (GB/T 50123-2019) [17], consolidation creep tests with different vertical loads (loading stresses) were carried out. The test instrument, shown in Figure 2, is GZQ-1 automatic pressure consolidation apparatus produced by Nanjing Ningxi Soil Instrument Co., LTD. The instrument has the advantages of stable system and low noise and the area of its ring knife is 30 cm^2, so the size of soil sample is 6.18 cm × 2.00 cm. In the process of cutting soil samples, attention should be paid to the balanced side-pressing and side-cutting operation of the original soil block so as to make the top surface of the soil sample flat without any holes.



Figure 2. Automatic pneumatic consolidation instrument (16 containers).

2.3. Testing Program

Firstly, manually input and proofread 14 test soil sample numbers and corresponding ring cutter numbers in the data acquisition system, and select and confirm the loading series and test methods. Then, in order to ensure the smooth progress of the test and the range of the displacement sensor, it is necessary to carry out zero correction operation, and confirm that the dial indicator pointer points to the 5–9 mm area. Finally, start the experiment and save the data file. In addition, set the program system to record data 12 times within one hour, and the data collection period after one hour is half an hour.

There are two loading methods for consolidation creep test, independent loading and graded loading, each of which has its own characteristics. Independent loading means different samples are loaded synchronously by using the same test instrument with the same test conditions and kept constant after loading. Graded loading is to load the sample until the deformation is stable, and then start the next load. In addition, the creep curve of

soil samples obtained by graded loading has the characteristics of a ladder (y values are constant for a range of x values, then increase to another level and remain for another range of x values), which cannot show the change law of soil creep directly. Considering the test instrument can control the container separately, and the influence of load superposition on the test results, the method of independent loading was chosen in the experiment.

According to the properties of soil, seven soil samples were selected from the two layers (No. III and No. IV soil layers) and numbered. The test lasted for 8 days. The soil samples in each group were set as vertical loads (σ) of 100 kPa, 200 kPa, 300 kPa, 400 kPa, 500 kPa, 600 kPa, and 700 kPa, respectively. The loading scheme was listed in Table 2.

Table 2. Experimental scheme for creep test of soil samples.

Soil Type	Number	Stress σ/kPa	Loading Method
Sandy soil (A)	A1	100	Independent loading
	A2	200	
	A3	300	
	A4	400	
	A5	500	
	A6	600	
	A7	700	
Silty clay (B)	B1	100	
	B2	200	
	B3	300	
	B4	400	
	B5	500	
	B6	600	
	B7	700	

It is worth noting that this study only discusses the construction process of the empirical model, so the accidental factor of the sample is not considered in the experimental design. In future studies, the number of samples will be expanded to conduct a more in-depth statistical analysis of the red loam creep test.

2.4. Experimental Results and Analysis

The creep test data were extracted and 26 data points within 10–100 min were selected for analysis (Table 3), and the constitutive relationship of strain and time as shown in Figure 3 was obtained.

Consolidation compression of soil is composed of primary consolidation and secondary consolidation. The deformation caused by secondary consolidation can be regarded as creep deformation during the process of consolidation compression creep test [18]. Figure 3 shows that a certain amount of deformation occurs at the beginning of loading, because the strain of sand increases linearly and rapidly with time going by, and the deformation is caused by the primary consolidation at the initial stage of loading. When σ = 100 kPa, 200 kPa, and 300 kPa, the deformation of sand shows a trend of steady and slowly increasing over time after a certain amount of strain appears at the initial loading stage. When σ = 400 kPa and 500 kPa, it showed the same pattern. However, the strain of sand in the later stage increased rapidly and nonlinearly, when σ = 600 kPa and 700 kPa. The initial value of the creep curve is regarded as the primary consolidation strain, and then the primary consolidation strain and creep strain under different stresses are counted, as shown in Table 4. As can be seen from Table 4, when the vertical load was 100 kPa, the creep strain of the soil sample was only 0.61%, and when the loading reached 700 kPa, it was 1.32%, indicating that the creep characteristics of Changsha sandy soil have structural effects.

Table 3. Test results of sandy soil.

Time (min) \ Stress (kPa) / Deformation (mm)	100	200	300	400	500	600	700
10	0.172	0.296	0.378	0.570	0.708	0.830	0.982
30	0.250	0.460	0.610	0.822	1.020	1.292	1.494
60	0.302	0.538	0.730	0.916	1.116	1.440	1.628
120	0.314	0.548	0.742	0.928	1.128	1.454	1.646
180	0.326	0.556	0.754	0.942	1.140	1.466	1.664
240	0.334	0.564	0.764	0.952	1.148	1.474	1.680
300	0.344	0.574	0.776	0.964	1.174	1.484	1.694
420	0.358	0.582	0.786	0.974	1.182	1.492	1.708
540	0.364	0.590	0.796	0.982	1.190	1.504	1.720
720	0.372	0.596	0.804	0.988	1.196	1.512	1.728
900	0.378	0.604	0.810	0.994	1.200	1.518	1.734
1440	0.386	0.610	0.814	0.998	1.204	1.524	1.738
2160	0.394	0.616	0.820	1.004	1.204	1.528	1.740
2880	0.402	0.622	0.826	1.010	1.206	1.530	1.742
3600	0.406	0.626	0.834	1.016	1.210	1.534	1.742
4320	0.410	0.632	0.840	1.022	1.214	1.538	1.746
5040	0.414	0.636	0.844	1.026	1.220	1.548	1.750
5760	0.422	0.640	0.848	1.030	1.226	1.554	1.758
6480	0.426	0.642	0.850	1.034	1.232	1.558	1.764
7200	0.428	0.644	0.854	1.036	1.236	1.564	1.772
7920	0.432	0.644	0.856	1.038	1.244	1.568	1.780
8640	0.434	0.646	0.862	1.042	1.252	1.574	1.788
9360	0.436	0.646	0.866	1.046	1.260	1.580	1.798
10,080	0.440	0.650	0.868	1.052	1.266	1.590	1.818
10,800	0.436	0.648	0.872	1.058	1.276	1.604	1.842
11,520	0.444	0.650	0.878	1.068	1.296	1.622	1.892

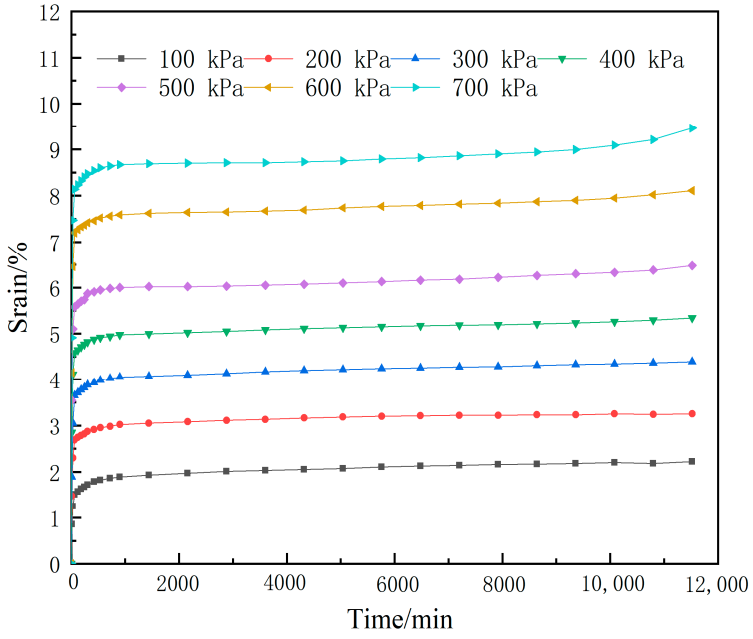


Figure 3. Strain–time curves of sandy soil with different vertical loads.

Table 4. Strain of sandy soil under different vertical loads.

Number	Stress σ/kPa	Total Strain ε/%	Primary Consolidation Strain ε_z/%	Creep Strain ε_c/%
A1	100	2.22	1.51	0.61
A2	200	3.25	2.69	0.56
A3	300	4.39	3.65	0.74
A4	400	5.34	4.58	0.76
A5	500	6.48	5.58	0.90
A6	600	8.11	6.93	1.18
A7	700	9.46	8.14	1.32

According to the test data listed in Table 5, the relationship between strain and time of silty clay under different vertical loads was obtained (Figure 4). It can be seen from Figure 4 that the silty clay has a similar phenomenon. When the vertical load was 100 kPa, the creep strain of the soil sample was 0.88%. When the loading reached 700 kPa, it increased to 1.58%, as shown in Table 6.

Table 5. Test results of silty clay.

Time (min) \ Stress (kPa) / Deformation (mm)	100	200	300	400	500	600	700
10	0.206	0.332	0.494	0.622	0.804	0.934	1.038
30	0.326	0.464	0.678	0.854	1.136	1.384	1.588
60	0.382	0.562	0.788	0.976	1.226	1.494	1.712
120	0.402	0.594	0.822	0.982	1.294	1.544	1.758
180	0.422	0.624	0.850	1.004	1.318	1.578	1.780
240	0.434	0.676	0.872	1.020	1.336	1.608	1.792
300	0.448	0.682	0.890	1.034	1.352	1.630	1.804
420	0.458	0.690	0.906	1.046	1.362	1.648	1.818
540	0.466	0.698	0.918	1.056	1.372	1.658	1.826
720	0.474	0.704	0.930	1.072	1.380	1.666	1.836
900	0.486	0.710	0.938	1.086	1.386	1.672	1.848
1440	0.492	0.716	0.944	1.102	1.390	1.676	1.856
2160	0.500	0.720	0.950	1.116	1.394	1.680	1.866
2880	0.508	0.722	0.954	1.128	1.402	1.686	1.872
3600	0.518	0.728	0.960	1.144	1.408	1.692	1.880
4320	0.522	0.736	0.966	1.150	1.414	1.698	1.890
5040	0.528	0.740	0.972	1.158	1.420	1.700	1.898
5760	0.532	0.746	0.976	1.168	1.422	1.704	1.906
6480	0.536	0.750	0.980	1.176	1.426	1.710	1.912
7200	0.544	0.752	0.986	1.184	1.430	1.714	1.918
7920	0.548	0.754	0.990	1.192	1.432	1.716	1.924
8640	0.544	0.754	0.994	1.200	1.432	1.722	1.930
9360	0.548	0.758	0.996	1.206	1.434	1.730	1.936
10,080	0.550	0.762	1.002	1.216	1.456	1.746	1.942
10,800	0.552	0.764	1.006	1.228	1.480	1.766	1.974
11,520	0.558	0.766	1.014	1.234	1.514	1.790	2.028

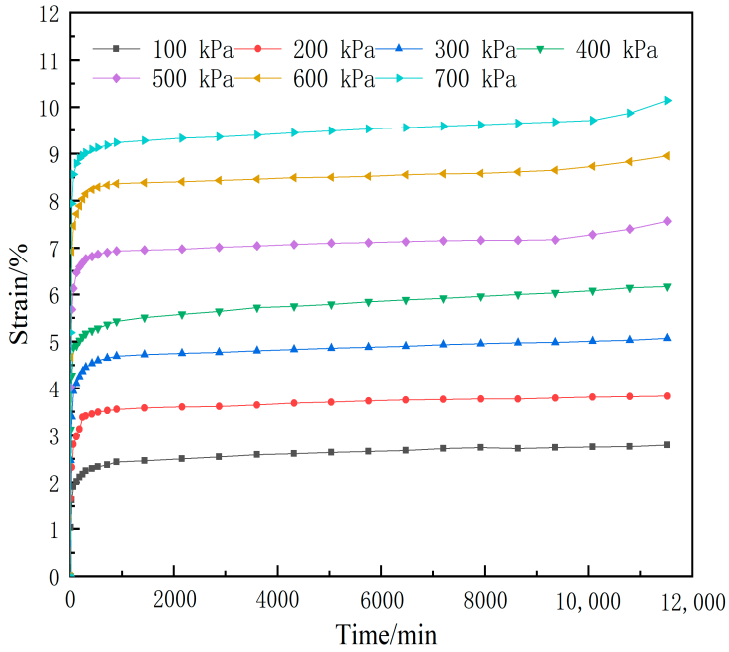


Figure 4. Strain–time curves of silty clay under different vertical loads.

Logarithmic coordinates were used instead of ordinary coordinates, as shown in Figure 5. As can be seen from Figure 5, the strain curves of both sandy soil and silty clay are broken lines, and the time corresponding to the inflection point of the broken line is t = 60 min, indicating that the primary consolidation process was completed in 1 h. According to Tables 4 and 6, the average deformation corresponding to the completion of primary consolidation in each group (A and B) is 82.47% and 78.22%, respectively.

Table 6. Strain of silty clay under different vertical loads.

Number	Stress σ/kPa	Total Strain ε/%	Primary Consolidation Strain ε_z/%	Creep Strain ε_c/%
B1	100	2.79	1.91	0.88
B2	200	3.83	2.81	1.02
B3	300	5.07	3.94	1.13
B4	400	6.17	4.88	1.29
B5	500	7.57	6.13	1.44
B6	600	8.95	7.47	1.48
B7	700	10.14	8.56	1.58

The relationship of the stress–creep strain curve of the soil sample is drawn based on the test data, as is shown in Figure 6. From Figure 6, it can be seen that the creep deformation of soil samples under confined loading conditions is positively correlated with loading stress. With the same experimental conditions, the creep deformation of silty clay is larger than that of sandy soil.

Figure 7 shows the isochronous curves of sandy soil and silty clay. It can be seen that the isochronous curves approach the longitudinal axis (strain axis) with the increase in time. After 60 min of loading, the corresponding curves at different times roughly coincide with each other, but the offset is small, indicating that the creep characteristics of soil samples become more obvious with the increase in time in the process of secondary consolidation.

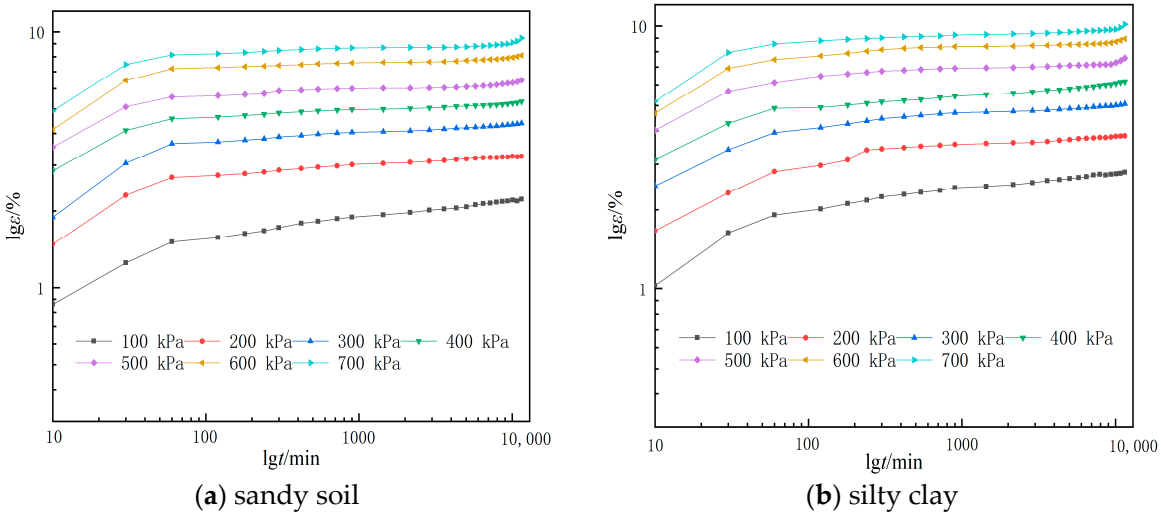


Figure 5. The strain–time curves of soil samples in logarithmic coordinates.

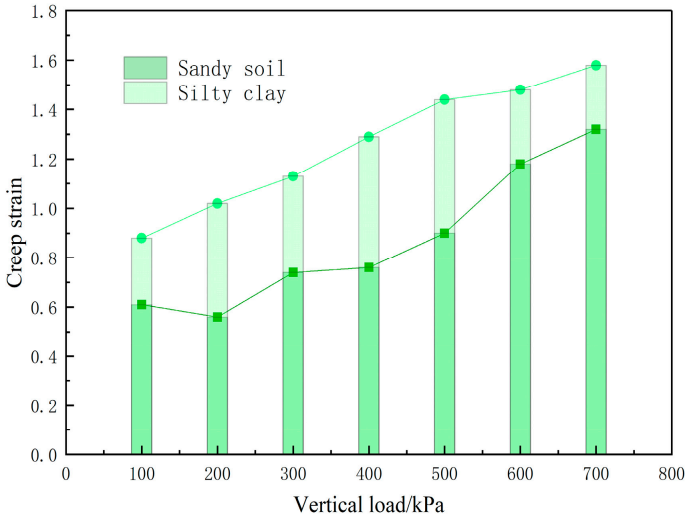
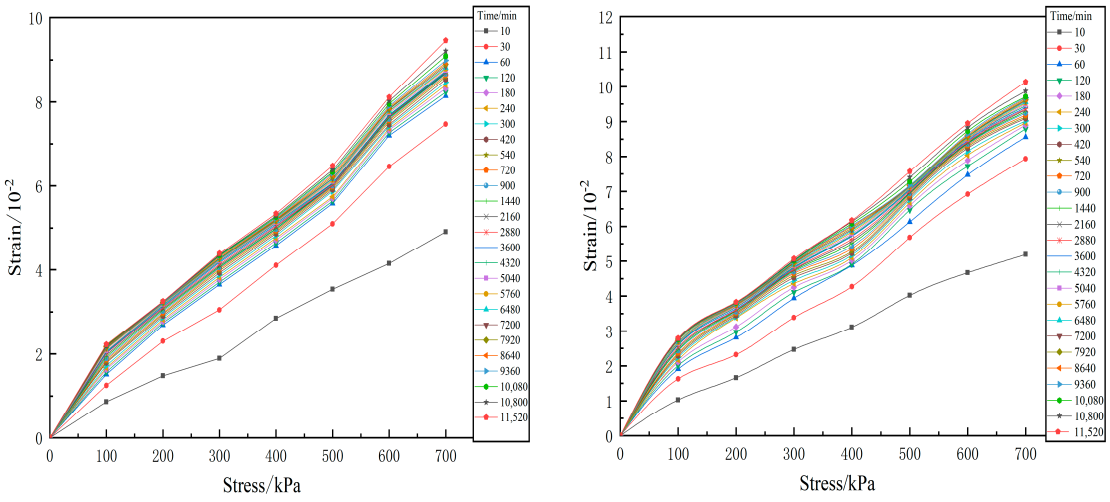


Figure 6. The stress–creep strain relationship curve of soil samples.

From the analysis above, it can be drawn that when the vertical load is less than 500 kPa, the creep process of soil samples shows transient deformation, decelerated creep, and constant creep, which reflects the viscoelastic and viscoplastic characteristics of the sandy soil and silty clay. When the vertical load is added to 500 kPa, transient deformation, decelerated creep, constant creep, and accelerated creep stages have occurred in the creep process, which reflects the nonlinear viscoelastic-plastic characteristics. In addition, in the consolidation creep test of sandy soil and silty clay in Changsha, the time of the completion of the primary consolidation is about 1 h, and then the transition to the creep stage of slow deformation.



(**a**) sandy soil (**b**) silty clay

Figure 7. Isochronous curve.

3. Empirical Creep Model Theory

The core idea of constructing an empirical creep model is to find out the relationship between the input variable (independent variable) and output variable (dependent variable) and establish a corresponding mathematical model by combining engineering practice and test data. According to reference [19], the relationship between stress, strain, and time in the creep constitutive model can be written as follows:

$$\varepsilon = f(\sigma, t) \tag{1}$$

$$\sigma = g(\varepsilon, t) \tag{2}$$

where σ represents loading stress, ε represents soil strain, and t represents time.

Equations (1) and (2) represent isochronous curves and creep curves, respectively. In terms of expression form, the isochronous curve is the σ-ε curve with a different time, and the creep curve is the ε-t curve under different stress. Based on the similarity of creep curves, similar conditions of creep curves can be obtained, as is shown in Equation (3).

$$\begin{gathered} g(\varepsilon, t) = \sigma\, g(\sigma\, , t) \\ \varepsilon(\sigma, t) = f(\sigma, t) g(\sigma, t) \end{gathered} \tag{3}$$

where $\varepsilon(\sigma, t)$ represents creep strain, ε represents soil strain, and t is time, $f(\sigma, t)$ represents the stress–strain relation function at time t, $g(\sigma, t)$ represents the strain–time function with different σ.

Singh–Mitchell Model was proposed by Singh A and Mitchell J.K in 1968, and used the combination form of power function and exponential function, respectively, to describe the creep characteristics of soil mass, where the power function represented the ε-t curve and the exponential function represented the σ-ε curve. The stress–strain–time relationship of this model is as follows:

$$\varepsilon = A_{\mathrm{r}} \left(\frac{t_{\mathrm{r}}}{t} \right)^{m} \mathrm{e}^{aD_{\mathrm{r}}} \tag{4}$$

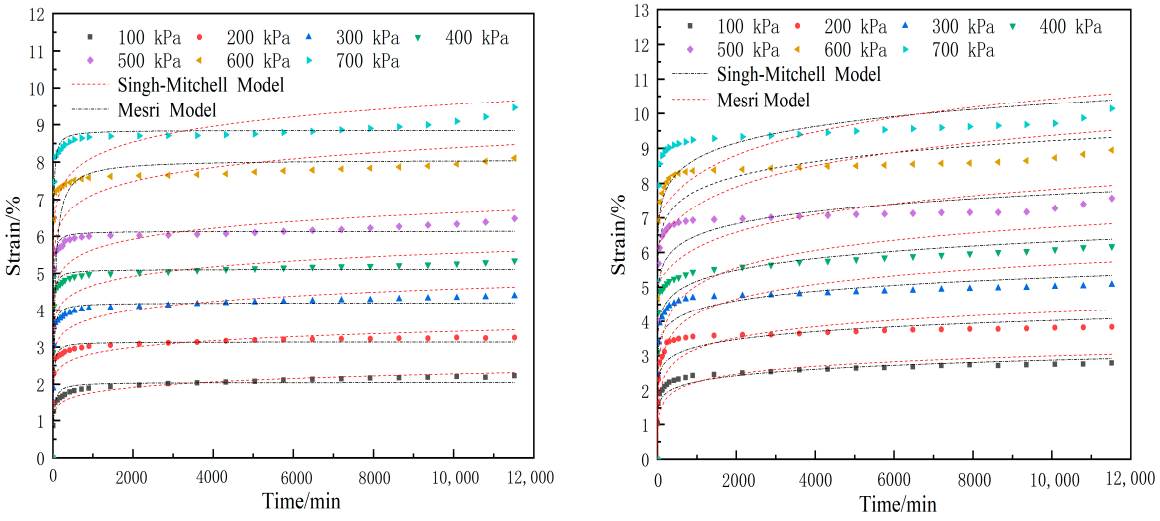
where D_{r} represents stress level, t_{r} represents reference time, and A_{r}, m, and a are model parameters.

The Mesri Model was proposed by Mesri in 1981, which used the power function and hyperbolic function, respectively, to represent curves and curves. The stress–strain–time relationship of this model is as follows:

$$\varepsilon = B_{\mathrm{r}} \frac{D_{\mathrm{r}}}{1 - bD_{\mathrm{r}}} \left(\frac{t}{t_{\mathrm{r}}} \right)^{n} \tag{5}$$

where B_{r}, b, and n are model parameters.

The empirical creep model has the advantages of simple form, convenient use, and few parameters, a large number of engineering practices and laboratory creep tests show that soil creep has nonlinear characteristics, which can be described by the empirical creep model [20–25]. Traditional empirical creep models (Singh–Mitchell Model and Mesri Model) were used to calculate the creep curve of Changsha red loam, as shown in Figure 8. It found that the creep curves calculated by the Singh–Mitchell Model and Mesri Model cannot describe the creep characteristics of Changsha red loam well. Therefore, the empirical creep constitutive model suitable for describing the creep characteristics of Changsha red loam is to be discussed.



(**a**) sandy soil (**b**) silty clay

Figure 8. Curve comparison between Changsha red loam creep test and traditional empirical model.

4. Establishment of Empirical Creep Constitutive Model

The curve straightening method (also known as the variable transformation method) is an efficient mathematical method to analyze test curves. By using the coordinate transformation, the curve is straighter and the curve relation is transformed from nonlinear to linear, aiming at analyzing test curves more easily [26]. By analyzing the variation law of the ε-t curve and the σ-ε curve, the creep data of 100 kPa, 200 kPa, 400 kPa, 500 kPa, and 700 kPa were selected as the analysis object, and then, appropriate nonlinear functions were selected to construct a suitable empirical creep model.

(1) Strain–time relationship

According to the study above, secondary consolidation deformation of Changsha sandy soil occurred 1 h later after loading. Extracting the creep test data from 60 to 11,520 min draws the lgε-lg$t$ curve in Figure 9. "Pearson's R" index was selected to judge the fitting effect of the curve. It can be seen from Figure 9 that the manifestation of creep curves in logarithmic coordinates is linear, and the fitting line has a high degree of coincidence with the experimental curve, with the correlation coefficients ranging from

0.9158 to 0.9951. On the basis of the lgε-lg$t$ curve, the relation between creep strain and time can be obtained as follows:

$$\lg g(\sigma, t) = \lg g(\sigma, t_0) + m(\lg t - \lg t_0) \tag{6}$$

where m represents the slope of the lgε-lg$t$ curve corresponding to the fitting line, t_0 is the reference time, in this creep model, t_0 is set at 60 min, $g(\sigma, t_0)$ and represents the creep strain at t_0 under different σ.

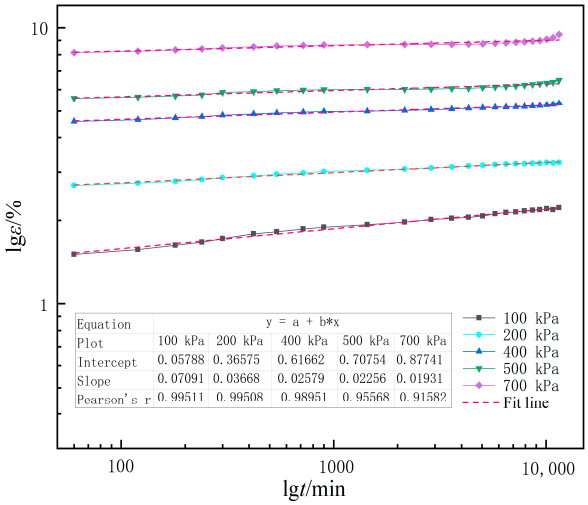


Figure 9. lgε-lg$t$ relation of Changsha sand soil and its linear fitting curve.

By converting equation, Equation (6) can be transformed into Equation (7) as follows:

$$g(\sigma, t) = g(\sigma, t_0)\left(\frac{t}{t_0}\right)^m \tag{7}$$

It can be seen from Equation (7) that it is more appropriate to describe the strain–time relationship of the sandy soil by the power function.

(2) Stress–strain relationship

Figure 10 shows the isochron curves of sandy soil strain at different times, it can be seen that lgσ and lgε have a good linear relationship, and the linear fitting effect is good, with the correlation coefficient being 0.9910–0.9979. According to the lgσ-lgε curve, the relation between stress and creep strain can be obtained as follows:

$$\lg f(\sigma, t) = \lg f(\sigma_0, t) + n(\lg\sigma - \lg\sigma_0) \tag{8}$$

where n represents the slope of the lgσ-lgε curve corresponding to the fitting line, σ_0 refers to reference stress, in this creep model, σ_0 is 100 kPa, $f(\sigma_0, t)$ and represents the creep strain at σ_0 with different t.

Through equation conversion, Equation (8) can be simplified to Equation (9) as follows:

$$f(\sigma, t) = f(\sigma_0, t)\left(\frac{\sigma}{\sigma_0}\right)^n \tag{9}$$

Equation (9) indicates that the stress–strain relationship of the sandy soil conforms to the power function relationship

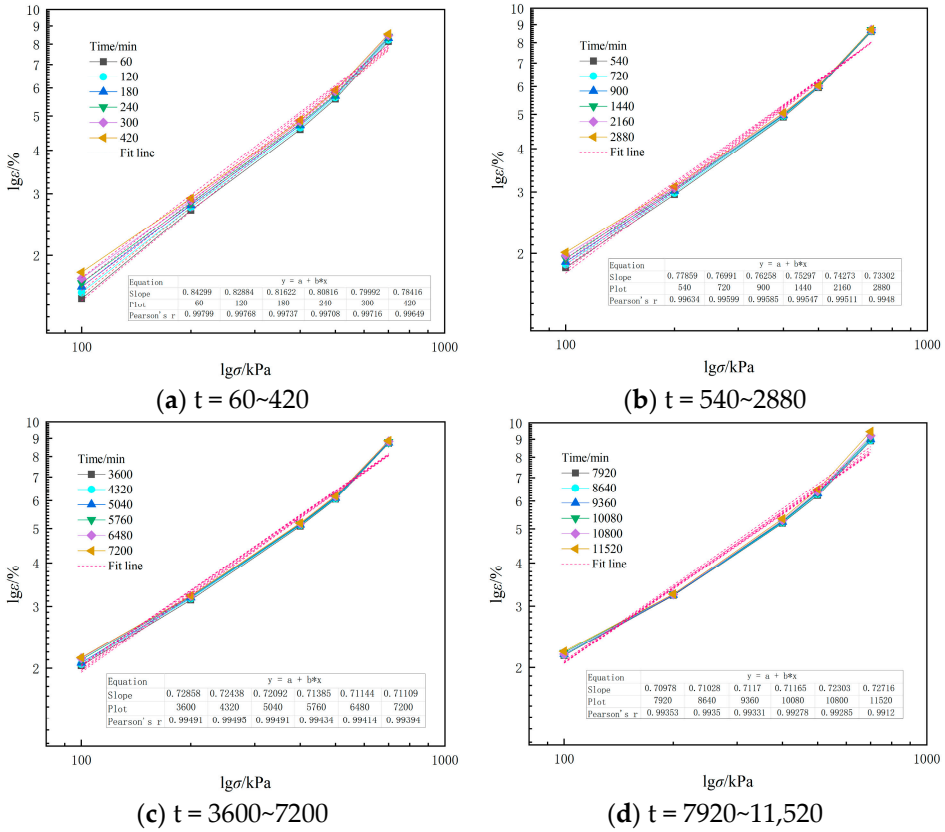


Figure 10. lgσ-lgε relation and its linear fitting curve of Changsha sandy soil at different times.

(3) Stress–strain–time relationship

Based on the analysis above, it is feasible to use the power function to express the ε-t curve and the σ-ε curve of sandy soil.

According to Equations (3), (7), and (9), Equation (10) can be obtained:

$$\begin{aligned} \varepsilon(\sigma, t) &= f(\sigma_0, t)\left(\frac{\sigma}{\sigma_0}\right)^n g(\sigma, t_0)\left(\frac{t}{t_0}\right)^m \\ &= \varepsilon(\sigma_0, t_0)\left(\frac{\sigma}{\sigma_0}\right)^n \left(\frac{t}{t_0}\right)^m \end{aligned} \tag{10}$$

Set $k = \varepsilon(\sigma_0, t_0)$, the empirical creep model of the sandy soil can be written as follows:

$$\varepsilon(\sigma, t) = k\left(\frac{\sigma}{\sigma_0}\right)^n \left(\frac{t}{t_0}\right)^m \tag{11}$$

where k, m, and n are parameters of the empirical creep model. k represents the strain by the condition of reference time and reference stress, which can be calculated by experimental data $\varepsilon(\sigma_0, t_0)$. m reflects the creep rate of soil, which can be obtained by solving the slope of the lgε-lg$t$ curve. n represents the compressive property of soil and can be obtained by calculating the slope of the lgσ-lgε curve.

Model parameter k was obtained by calculating $\varepsilon(100\ \text{kPa}, 60\ \text{min})$ on the basis of the test data (Table 3). Considering the lgε-lg$t$ relation of sandy soil, the slopes of different curves were obtained by linear fitting (Table 7), then parameter m was obtained by calculating the average value of fitting parameters. The average value of the fitting parameters, obtained from the lgσ-lgε relation in Table 8, was used to calculate the parameter n. Parameters of the empirical creep model of sandy soil are shown in Table 9.

Table 7. Fitting parameters of lgε-lg*t* relation of Changsha sandy soil.

Press σ/kPa	Fitting Parameters	Correlation Index
100	0.0709	0.9951
200	0.0367	0.9951
400	0.0258	0.9895
500	0.0226	0.9557
700	0.0193	0.9158

Table 8. Fitting parameters of lgσ-lgε relation of Changsha sandy soil.

Time *t*/min	Fitting Parameters	Correlation Index	Time *t*/min	Fitting Parameters	Correlation Index
60	0.8430	0.9980	3600	0.7286	0.9949
120	0.8288	0.9977	4320	0.7244	0.9950
180	0.8162	0.9974	5040	0.7209	0.9949
240	0.8082	0.9971	5760	0.7139	0.9943
300	0.7999	0.9972	6480	0.7114	0.9941
420	0.7842	0.9965	7200	0.7111	0.9939
540	0.7786	0.9963	7920	0.7098	0.9935
720	0.7699	0.9960	8640	0.7103	0.9935
900	0.7626	0.9959	9360	0.7117	0.9933
1440	0.7530	0.9955	10,080	0.7117	0.9928
2160	0.7427	0.9951	10,800	0.7230	0.9929
2880	0.7330	0.9948	11,520	0.7272	0.9912

Table 9. Parameters of empirical creep model of sandy soil in Changsha.

Soil Layer	*k*	*m*	*n*
No. III Sandy soil	1.5100	0.0351	0.7510

5. Model Verification and Application

Not only can a good model reflect some corresponding relationships in the prototype, but it also will have good application and extension performance. In order to verify the rationality and accuracy of the empirical creep model of the sandy soil, the creep curves under vertical loads of 300 kPa and 600 kPa were predicted based on the established empirical creep model. The prediction results of the model are shown in Figure 11.

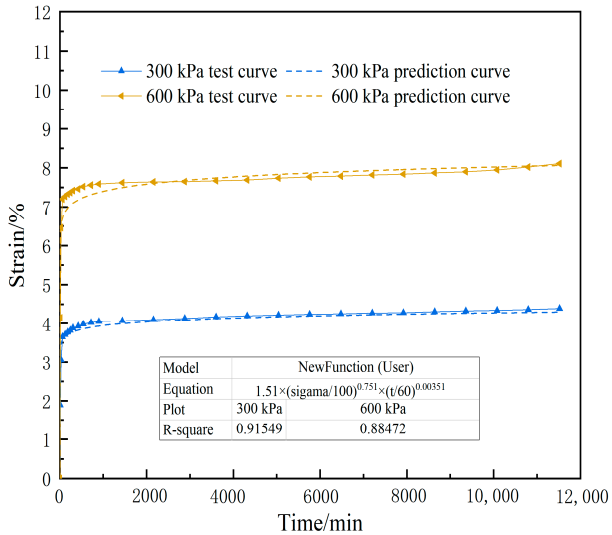


Figure 11. Comparison between prediction curve and test curve of sandy soil.

As can be seen from Figure 11, the prediction curve under 300 kPa is in good agreement with the test curve, and the goodness of fit (R^2) is 0.9155. The reason why, when the vertical load was 600 kPa, the anastomosis effect was slightly worse than that of 300 kPa is that the accelerated creep stage appeared in the creep curve under this load. The prediction results show that the empirical creep model can predict the creep curve of the sandy soil with high fitting accuracy.

In a similar way, the model is used to predict the creep deformation of silty clay. Based on the creep test data of the silty clay (Table 5), the model parameters k, m, and n can be obtained by analyzing the lgε-lg$t$ and lgσ-lgε curves corresponding to 100 kPa, 300 kPa, 500 kPa, and 700 kPa, as seen in Tables 10–12. According to the model parameters in Table 12, the empirical creep model is established to predict the creep curves of silty clay under vertical loads of 200 kPa, 400 kPa, and 600 kPa. The prediction results are shown in Figure 12.

Table 10. Fitting parameters of lgε-lg$t$ relation of Changsha silty clay.

Press σ/kPa	Fitting Parameters	Correlation Index
100	0.0971	0.9641
300	0.0666	0.9386
500	0.0493	0.9083
700	0.0480	0.8825

Table 11. Fitting parameters of lgσ-lgε relation of Changsha silty clay.

Time t/min	Fitting Parameters	Correlation Index	Time t/min	Fitting Parameters	Correlation Index
60	0.7820	0.9829	3600	0.6719	0.9808
120	0.7692	0.9806	4320	0.6693	0.9811
180	0.7491	0.9805	5040	0.6654	0.9809
240	0.7294	0.9826	5760	0.6627	0.9813
300	0.7201	0.9816	6480	0.6606	0.9813
420	0.7136	0.9811	7200	0.6555	0.9801
540	0.7073	0.9811	7920	0.6533	0.9799
720	0.7019	0.9819	8640	0.6583	0.9816
900	0.6930	0.9811	9360	0.6563	0.9810
1440	0.6887	0.9822	10,080	0.6587	0.9819
2160	0.6834	0.9820	10,800	0.6659	0.9811
2880	0.6789	0.9813	11,520	0.6736	0.9780

Table 12. Parameters of empirical creep model of silty clay in Changsha.

Soil Layer	k	m	n
No. IV Silty clay	1.9100	0.0653	0.6903

As can be seen from Figure 12, when σ = 200 kPa and 400 kPa, the predicted curves were in good agreement with the creep test curves, with R^2 being 0.9244 and 0.9638, respectively. When σ = 600 kPa, the predicted curve of the model was not in good agreement with the creep test curve, and the R^2 was 0.8916. The reason is that silty clay exhibits a nonlinear creep phase under stresses of over 500 kPa. The prediction results indicate that the empirical creep model can predict the creep curve well and the fitting accuracy is high in a certain range of load. It can also be seen from Figures 10 and 11 that the predicted value is less than the measured value of creep at the initial stage of creep (decelerated creep stage), but it is greater when at the middle and late creep stage (steady speed stage and accelerated stage). It indicates that the model may do a poor job of predicting in the accelerated creep stage.

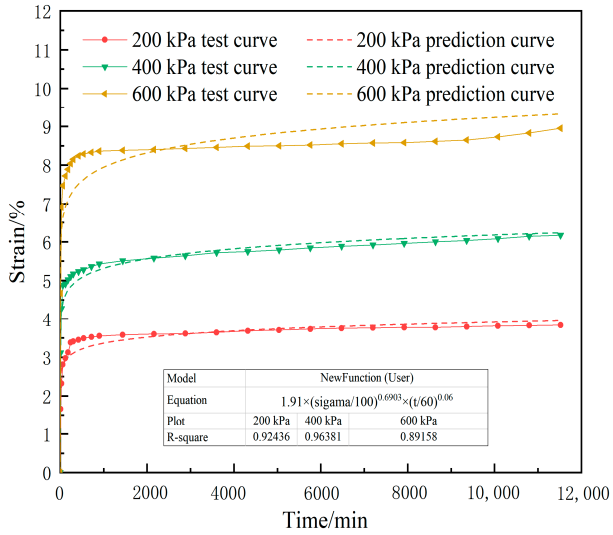


Figure 12. Comparison between prediction curve and test curve of silty clay.

From the analysis above, the empirical creep model is perfectly suitable for predicting the creep curves of sandy soil and silty clay in Changsha with loads less than 500 kPa, while the description of the accelerated creep behavior of red loam needs to be further studied.

6. Conclusions

Consolidation creep tests were carried out to propose an empirical model describing and predicting perfectly the creep characteristics of Changsha red loam. Conclusions are as follows.

First, the creep deformation of Changsha red loam changes with the vertical load. The deformation process illustrates deceleration and stabilization creep with its vertical load lower than 500 kPa, while it may illustrate acceleration with its vertical load higher than 500 kPa.

Second, the empirical creep model of Changsha red loam is described by a power function. Within 500 kPa, the empirical creep model reflects the nonlinear creep characteristics of sandy soil and silty clay well.

Third, the model above is applied to predicting the creep deformation of Changsha red loam, providing theoretical guidance for the creep deformation of soil under similar conditions.

Author Contributions: L.L. drafted the paper and performed the study, and Z.L. and Y.L. made important improvements to this paper. All authors have read and agreed to the published version of the manuscript.

Funding: This research was funded by [the National Natural Science Foundation of China] grant number [51708433].

Data Availability Statement: The data presented in this study are available on request from the corresponding author.

Acknowledgments: Project (No. 51708433) supported by the National Natural Science Foundation of China.

Conflicts of Interest: The authors declare no conflict of interest.

References

1. Huang, W.X. *Engineering Properties of Soil*; Water Resources and Electric Power Press: Beijing, China, 1983.
2. Li, A.; Deng, H.; Zhang, H.; Jiang, M.; Liu, H.; Xiao, Y.; Wen, J. Developing a two-step improved damage creep constitutive model based on soft rock saturation-loss cycle triaxial creep test. *Nat. Hazards* **2021**, *108*, 2265–2281. [CrossRef]
3. Long, M.; Grimstad, G.; Trafford, A. Prediction of embankment settlement on Swedish peat using the Soft Soil Creep model. *Proc. Inst. Civ. Eng.-Geotech. Eng.* **2020**, *175*, 507–522. [CrossRef]
4. Ofrikhter, V.G.; Ofrikhter, Y.V. Prediction of stress-strain state of municipal solid waste with application of soft soil creep model. *Vestn. MGSU* **2017**, *9*, 82–92.
5. Huang, W.; Wen, K.; Deng, X.; Li, J.; Jiang, Z.; Li, Y.; Li, L.; Amini, F. Constitutive model of lateral unloading creep of soft soil under excess pore water pressure. *Math. Probl. Eng.* **2020**, *2020*, 5017546. [CrossRef]
6. Zhang, Z.; Huang, C.; Jin, H.; Feng, W.; Jin, D.; Zhang, G. A creep model for frozen soil based on the fractional Kelvin-Voigt's model. *Acta Geotech.* **2022**, *17*, 4377–4393. [CrossRef]
7. Wang, P.; Liu, E.; Zhi, B.; Song, B.; Kang, J. Creep characteristics and unified macro–meso creep model for saturated frozen soil under constant/variable temperature conditions. *Acta Geotech.* **2022**, *17*, 5299–5319. [CrossRef]
8. Hou, F.; Lai, Y.; Liu, E.; Luo, H.; Liu, X. A creep constitutive model for frozen soils with different contents of coarse grains. *Cold Reg. Sci. Technol.* **2018**, *145*, 119–126. [CrossRef]
9. Hu, Z.Q.; Wang, K.; Li, H.R.; Liang, Z.C.; Jiao, H.W.; Wu, P.; Chen, Z.P. Nonlinear creep constitutive model for artificially prepared site soil. *Chin. J. Geotech. Eng.* **2021**, *43*, 13–18.
10. Yu, H.D.; Cui, J.C.; Chen, W.Z. Characterization of the long-term hydro-mechanical response in the host rock of a potential nuclear waste disposal repository. *Chin. J. Rock Mech. Eng.* **2022**, *41*, 2639–2648.
11. Liu, J.; Tang, Y.; Yi, L.; Peng, Y.C.; Zhou, Y.F. Creep Constitutive Model of Cobbly Soil and Its Engineering Application. *J. Yangtze River Sci. Res. Inst.* **2022**, *39*, 107–112.
12. Chen, C.F.; Liu, J.B.; Xu, Y.L.; Zhang, G.B. Tests on shearing creep of anchor-soil interface and its empirical model. *Chin. J. Geotech. Eng.* **2016**, *38*, 1762–1768.
13. Singh, A.; Mitchell, J.K. General stress-strain-time function for soils. *Geotech. Spec. Publ. ASCE* **1968**, *94*, 21–46. [CrossRef]
14. Mesri, G.R.E.S.; Febres-Cordero, E.; Shields, D.; Castro, A. Shear stress-strain-time behavior of clays. *Géotechnique* **1981**, *31*, 537–552. [CrossRef]
15. Long, L.; Li, Z.D. An assessment model of monitoring risk in deep excavation based on fuzzy theory. *Indoor Built Environ.* **2020**, *29*, 221–229. [CrossRef]
16. Long, L.; Li, Z.D. Monitoring and deformation law research of a deep foundation pit project in Changsha. *Build. Struct.* **2020**, *50*, 133–137.
17. *GB/T 50123-2019*; Standard for Geotechnical Test Methods. China Planning Press: Beijing, China, 2019.
18. Chen, X.P.; Zhu, H.H.; Zhang, F.Z.; Zhang, B. Experimental study on time dependent deformation of soft soil. *Chin. J. Rock Mech. Eng.* **2005**, *24*, 2142–2148.
19. Jing, G.; Li, S.; Chen, G.; Wei, J.; Sun, S.; Zhang, J. Research on creep test of compacted graphite cast iron and parameter identification of constitutive model under wide range of temperature and Stress. *Appl. Sci.* **2022**, *12*, 5032. [CrossRef]
20. Bobyleva, T.S.; Ma, W.G.; Yang, K.X. One-dimensional compression creep characteristics of light weight soil mixed with Weihe River mud and EPS particles. *Geotech. Geol. Eng.* **2021**, *39*, 4341–4353.
21. Bobyleva, T.N.; Shamaev, A.S. An efficient algorithm for calculating rheological parameters of layered soil media composed from elastic-creeping materials. *Soil Mech. Found. Eng.* **2017**, *54*, 224–230. [CrossRef]
22. Zou, S.; Li, J.; Xie, X.; Wang, Z. Study of the 1-D consolidation behavior of two-layered soft soils: Parametric studies using a rheological model with viscoplastic body. *Int. J. Numer. Anal. Methods Geomech.* **2019**, *43*, 501–518. [CrossRef]
23. Han, K.Y.; Liu, Q.; Song, X.D. Research on tests of the influence factors on creep property of sandy slate coarsegrained soil. *J. Railw. Eng. Soc.* **2014**, *11*, 63–67.
24. Zhu, Y.B.; Yu, H.M. Unsaturated creep behaviors of weak intercalated soils in soft rock of Badong formation. *J. Mt. Sci.* **2015**, *12*, 1460–1470. [CrossRef]
25. Cai, Y.; Chen, Y.; Cao, Z.; Ren, C. A combined method to predict the long-term settlements of roads on soft soil under cyclic traffic. *Acta Geotech.* **2018**, *13*, 1215–1226. [CrossRef]
26. Liao, H.Y.; Wang, W.; Gao, Y. Experimental study on creep characteristics of slip soil. *J. Chengdu Univ. (Nat. Sci.)* **2016**, *35*, 90–94.

Disclaimer/Publisher's Note: The statements, opinions and data contained in all publications are solely those of the individual author(s) and contributor(s) and not of MDPI and/or the editor(s). MDPI and/or the editor(s) disclaim responsibility for any injury to people or property resulting from any ideas, methods, instructions or products referred to in the content.